

Cell Reports, Volume 23

Supplemental Information

Nicotinic Cholinergic Receptors in VTA Glutamate

Neurons Modulate Excitatory Transmission

Yijin Yan, Can Peng, Matthew C. Arvin, Xiao-Tao Jin, Veronica J. Kim, Matthew D. Ramsey, Yong Wang, Sambashiva Banala, David L. Wokosin, J. Michael McIntosh, Luke D. Lavis, and Ryan M. Drenan

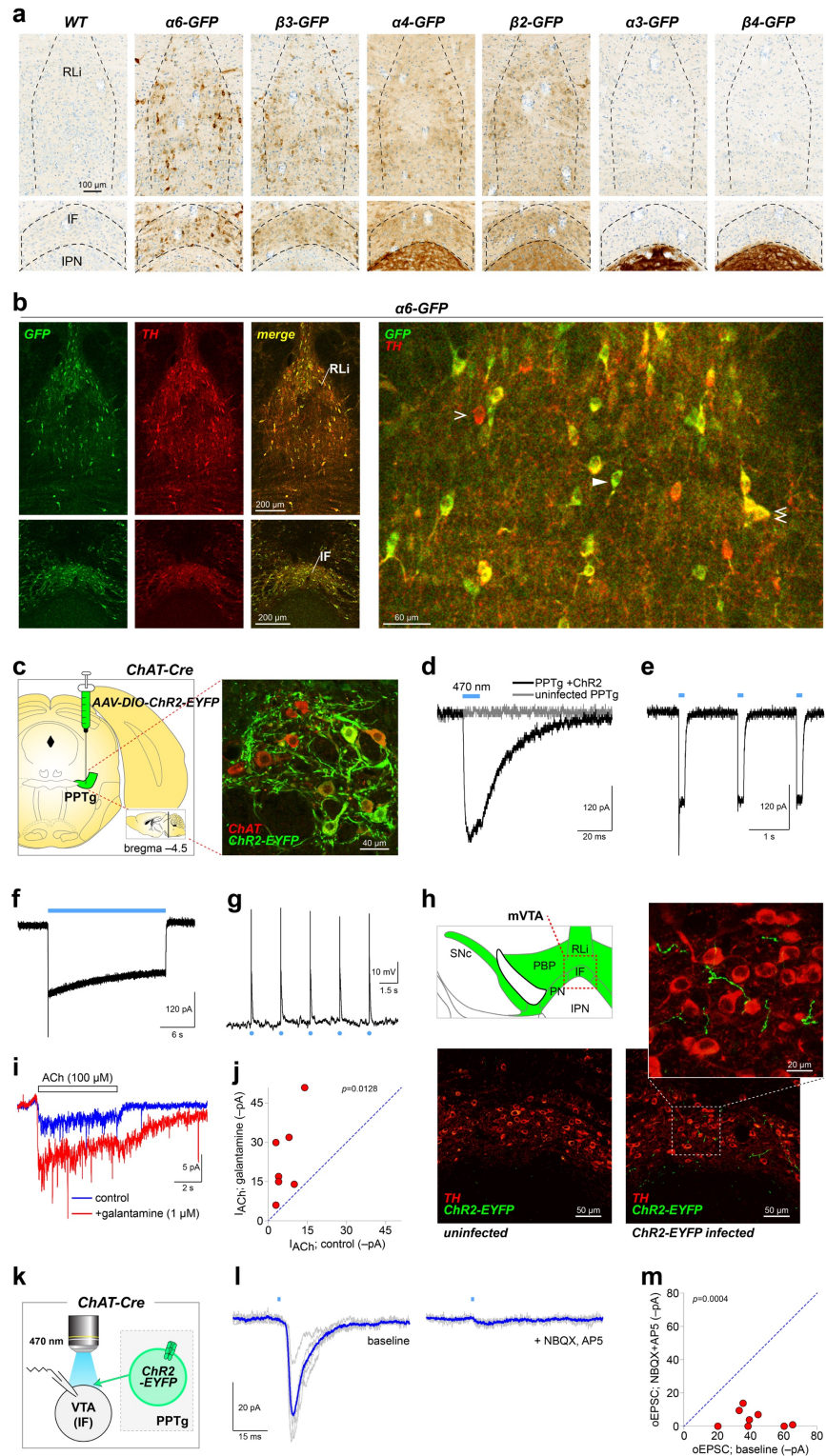


Figure S1. Related to Figure 1 – Supplemental data and opsin validation controls. (a) mVTA nuclei express nAChRs. Coronal sections containing mVTA structures (RLi: rostral linear nucleus; IF: interfasicular nucleus) dorsal to the interpeduncular nucleus (IPN) from knock-in/transgenic mice expressing the indicated GFP-fused nAChR subunit were stained with anti-GFP antibodies and visualized with DAB staining. Representative of $n=3$ mice. (b) The RLi and IF in coronal sections from $\alpha 6$ -GFP mice were co-stained with anti-GFP and anti-tyrosine

hydroxylase (TH) antibodies (left panels). A high-magnification image through the RLi is shown (right panel), with TH+/ $\alpha6^-$ (single open arrowhead), TH-/ $\alpha6^+$ (single closed arrowhead), and TH+/ $\alpha6^+$ neurons (double open arrowhead). (c) AAVs directing Cre-dependent expression of ChR2-EYFP were bilaterally injected into PPTg of ChAT-Cre mice at the approximate location indicated (left panel). Coronal sections from infected animals were stained with anti-ChAT and anti-GFP antibodies (right panel) to verify ChR2 expression in ChAT neurons. (d-f) Photocurrents were recorded in voltage-clamped PPTg neurons expressing ChR2. Brief (10 ms), intermediate (100 ms), and prolonged (20 s) light (470 nm, 0.12 mW/mm²) pulses demonstrate ChR2 functionality. (g) ChR2 activation drives action potential firing. A ChR2-expressing PPTg ChAT neuron was held in current clamp ($I=0$) configuration and repetitively stimulated with brief (0.1 ms) light flashes (0.12 mW/mm²) to elicit action potentials. (h) Expression of ChR2 in mVTA fibers. Coronal sections containing mVTA (top left; SNc: substantia nigra pars compacta, PBP: parabrachial pigmented nucleus, PN: paranigral nucleus, IF: interfascicular nucleus, RLi: rostral linear nucleus) from ChAT-Cre mice infected as described in (c) were stained with anti-TH and anti-GFP antibodies to visualize ChR2 expression in cholinergic fibers (top/bottom right). Specificity of detection is provided via uninfected control sections (bottom left). (i,j) Galantamine validation. Voltage-clamped mVTA glutamate neurons ($n=7$ cells/3 mice) were stimulated with pressure ejection application of ACh (100 μ M, 5 s, 1-2 psi) to mimic ChR2-mediated ACh release kinetics (Fig. 1f). Addition of galantamine potentiated ACh-evoked currents (i). (j) Plot for individual VTA glutamate neurons showing ACh-evoked current amplitude before (control) and after galantamine bath application. *P* value: two-sided paired *t*-test. (k) AAV-ChR2-EYFP vectors were microinjected into PPTg to express ChR2 non-specifically in this nucleus. Optical EPSCs (oEPSCs) were recorded in IF VTA neurons; results in (l,m). (l) oEPSCs in an IF VTA neuron before and after addition of NBQX (10 μ M) + D-AP5 (20 μ M). Individual sweeps (grey traces) and an average trace (blue trace) are shown. Representative of ($n=8$ cells/3 mice). (m) Plot for individual IF VTA neurons showing oEPSC amplitude before (baseline) and after bath application of NBQX (10 μ M) + D-AP5 (20 μ M). *P* value: two-sided paired *t*-test.

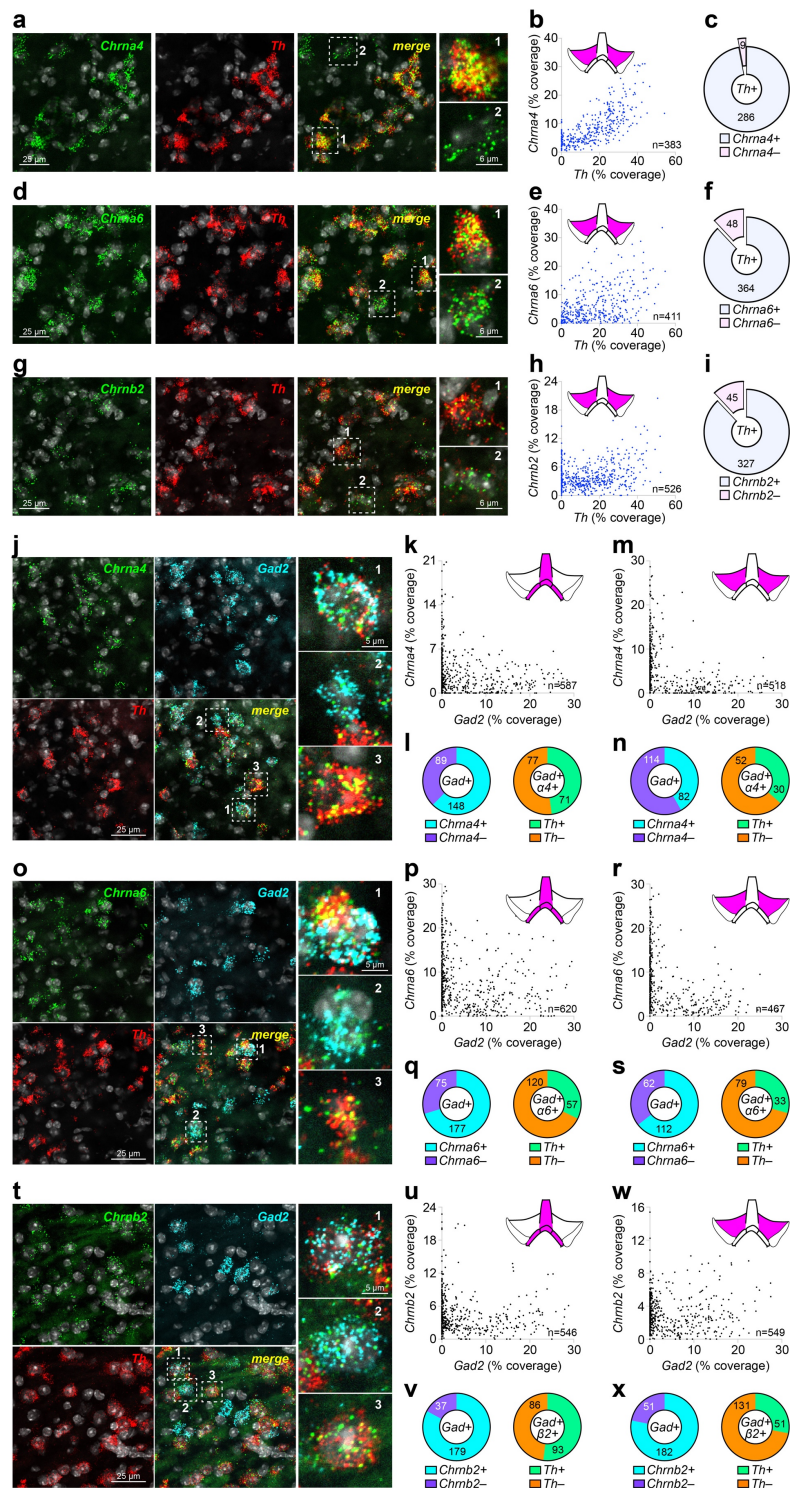


Figure S2. Related to Figure 2 – Supplemental FISH controls and data. (a-c) *Chrna4* FISH probe validation. (a) Representative 2-channel fluorescence *in situ* hybridization (FISH) images in lateral VTA neurons for probes: *Chrna4*, *Th*. Single *Chrna4*⁺ neurons indicated in the 'merge' panel, and shown enlarged (right panels), had this expression profile: 1) *Chrna4*⁺/*Th*⁺; 2) *Chrna4*⁺/*Th*⁻. (b-c) Analysis of *Chrna4*/*Th* co-expression in lateral VTA. (b) Scatter plots showing *Th* (abscissa) and *Chrna4* (ordinate) '% coverage' for all analyzed neurons. (c) Pie graph showing the fraction of *Th*⁺ neurons that were *Chrna4*⁺ vs. *Chrna4*⁻. (d-f) *Chrna6* FISH probe validation. Analysis

for *Chrna6* were performed as for *Chrna4*. **(g-i)** *Chrnb2* FISH probe validation. Analysis for *Chrnb2* were performed as for *Chrna4* and *Chrna6*. Data are pooled from n=3 mice. **(j-n)** Co-expression of *Chrna4* and *Gad2* in VTA neurons. **(j)** Representative 3-channel fluorescence *in situ* hybridization (FISH) images in mVTA neurons for the following probes: *Chrna4*, *Gad2*, and *Th*. Single *Chrna4*⁺ neurons indicated in the 'merge' panel, and shown enlarged (right panels), had this expression profile: 1) *Chrna4*⁺/*Gad2*⁺/*Th*⁺; 2) *Chrna4*⁺/*Gad2*⁺/*Th*⁻; 3) *Chrna4*⁺/*Gad2*⁻/*Th*⁺. **(k-l)** Analysis of *Chrna4*/*Gad2* co-expression in mVTA. **(k)** Scatter plots showing *Gad2* (abscissa) and *Chrna4* (ordinate) '% coverage' for all analyzed neurons. **(l)** Left: Pie graph showing the fraction of *Gad2*⁺ neurons that were *Chrna4*⁺ vs. *Chrna4*⁻. Right: *Th* expression status is shown for *Gad2*⁺/*Chrna4*⁺ neurons from left graph. **(m-n)** Analysis of *Chrna4*/*Gad2* co-expression in lateral VTA was performed as in mVTA (k-l). **(o-s)** Co-expression of *Chrna6* and *Gad2* in VTA neurons. Analysis for *Chrna6* were performed as for *Chrna4*. **(t-x)** Co-expression of *Chrnb2* and *Gad2* in VTA neurons. Analysis for *Chrnb2* were performed as for *Chrna4* and *Chrna6*. Complete data for nAChR/*Gad2* FISH is listed in **Table S2**. Data are pooled from n=3 mice.

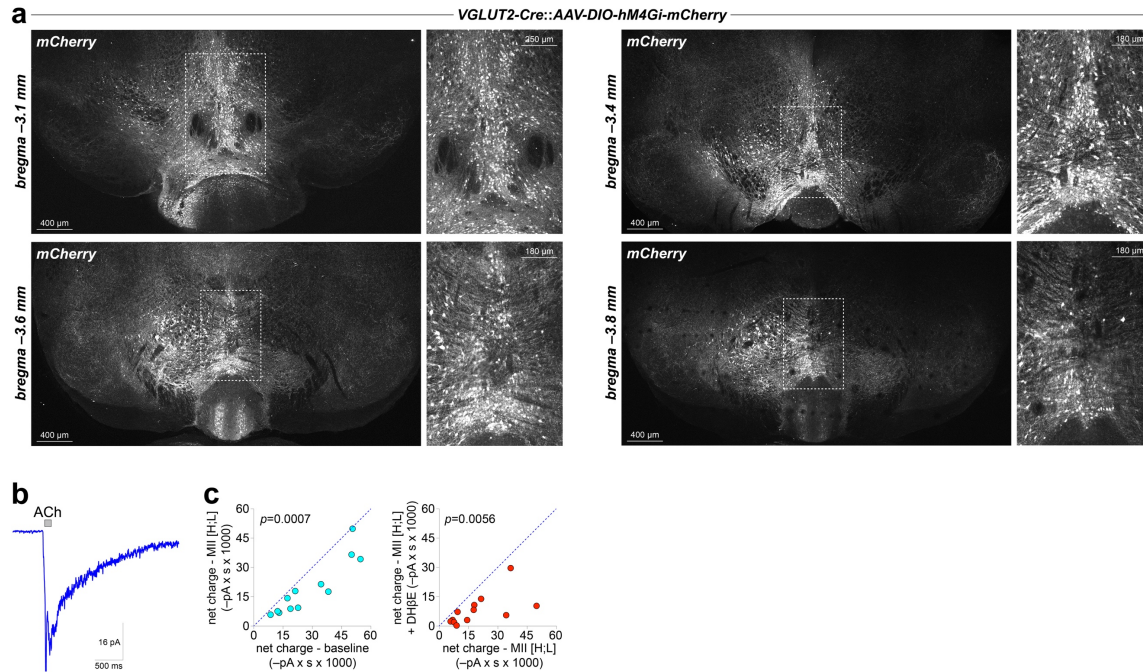


Figure S3. Related to Figure 3 – Controls for functional nAChR measurements in VGLUT2+ neurons. (a) Widefield images of ventral midbrain in VGLUT2-Cre mice microinjected in mVTA with AAV-DIO-hM4Gi-mCherry viral constructs. Anti-DsRed immunostaining was performed on coronal sections at the indicated bregma level. Boxed areas are shown enlarged immediately at right. Representative of $n>70$ mice. Micrograph for bregma -3.4 mm is also shown in **Fig. 3** in color and at higher zoom; it was shown here to allow a complete disclosure of hM4Gi-mCherry expression across the rostral-caudal extent of the VTA. **(b)** Averaged trace for pressure ejection applications of 1 mM ACh to mVTA neurons in slices from unlabeled/non-Cre C57BL/6 mice. **(c)** Left: 1 mM ACh-induced net charge at baseline vs. after bath application of α -Ctx MII[H9A;L15A] for ($n=9$ cells/5 mice) mVTA neurons from unlabeled/non-Cre C57BL/6 mice. Right: 1 mM ACh-induced net charge in the presence of α -Ctx MII[H9A;L15A] vs. α -Ctx MII[H9A;L15A] + 1 μ M DH β E for the same neurons shown at left. P values: two-sided paired t -test.

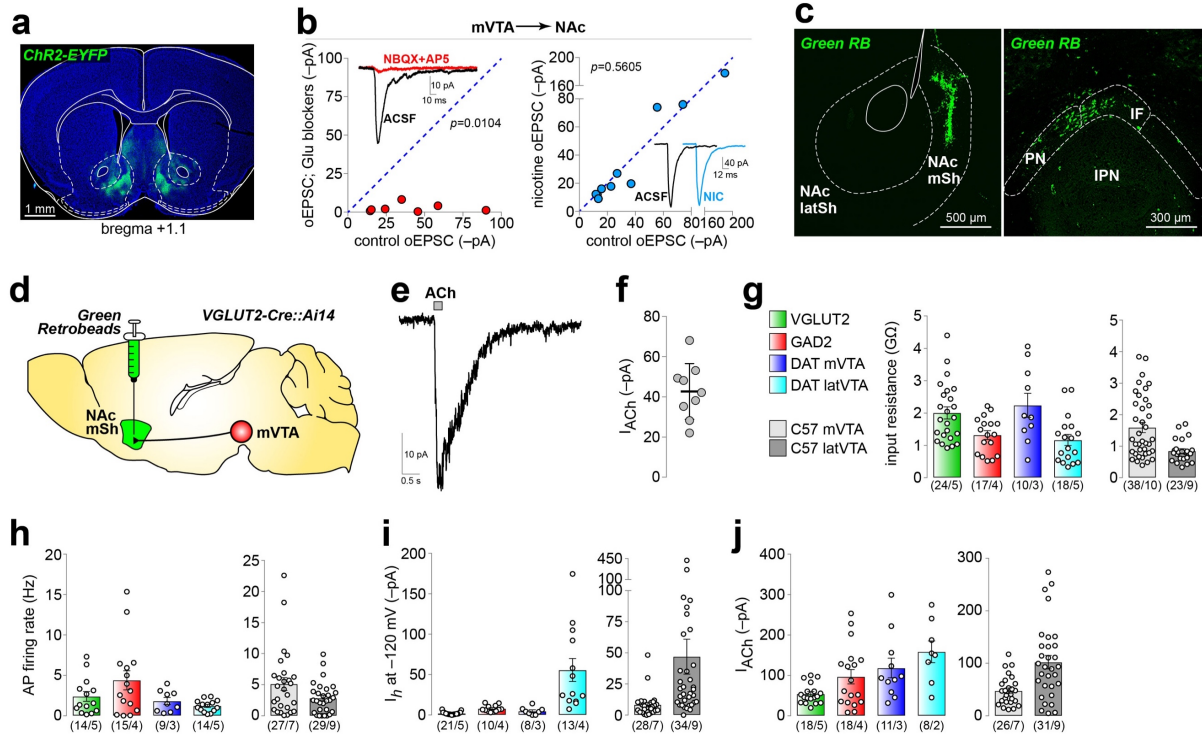


Figure S4. Related to Figure 4 - NAc glutamate transmission and electrophysiological properties of midbrain neurons. (a) ChR2-EYFP expression in NAc medial shell after ChR2 virus microinjection into mVTA of VGLUT2-Cre mice. (b) Sensitivity of NAc oEPSCs to NBQX + D-AP5 (left; $n=7$ cells/3 mice). Summary data for NAc oEPSCs before/after nicotine ($0.3 \mu\text{M}$) bath application (right; $n=10/5$). P values: two-sided paired t -test. (c) Green retrobead injection site in NAc medial shell (left) and resulting labeled mVTA neurons (right). (d) Green retrobeads were injected into NAc medial shell of VGLUT2-Cre::Ai14 mice. (e-f) ACh (1 mM)-evoked currents were measured in mVTA neurons with dual green+red fluorescence (representative trace (e) and scatter plot (f) of all response amplitudes (mean \pm s.d.; $n=9/2$). (g-j) Electrophysiological properties of mVTA neurons. Input resistance (g), action potential firing rate (h), I_h current at a holding potential of -120 mV (i), and peak current evoked by pressure ejection application of ACh (1 mM) (j) was measured in mVTA VGLUT2+, GAD2+, and DAT+ neurons in mVTA. DAT+ neurons in lateral VTA were also studied for comparison. The same properties were also measured in medial and lateral VTA neurons in slices from C57BL/6 WT mice. Number of cells and mice are indicated.

Table S1. Related to Figure 2 – Expression of *Chrna4*, *Chrna6*, and *Chrb2* in VTA glutamate neurons. Full quantification of triple channel mRNA FISH experiments is shown for medial (top section) and lateral VTA (bottom section). All sections were probed for *Slc17a6* and *Th*, while either *Chrna4*, *Chrna6* or *Chrb2* was probed in the 3rd channel.

| Medial VTA | | | | | | | | | | | | |
|-------------|-------|------------|------------|------------|-----------|-----------|-----------|------------|-----------|-----------|-----------|--|
| | Total | Slc17a6(+) | Slc17a6(-) | Slc17a6(+) | | | | Slc17a6(-) | | | | |
| | | | | TH(+) | TH(-) | TH(+) | TH(-) | TH(+) | TH(-) | TH(+) | TH(-) | |
| | | | | Chrna4(+) | Chrna4(+) | Chrna4(-) | Chrna4(-) | Chrna4(+) | Chrna4(+) | Chrna4(-) | Chrna4(-) | |
| # cells-> | 443 | 257/443 | 186/443 | 138/257 | 71/257 | 11/257 | 37/257 | 153/186 | 21/186 | 7/186 | 5/186 | |
| fraction-> | | 0.58 | 0.42 | 0.54 | 0.28 | 0.04 | 0.14 | 0.82 | 0.11 | 0.04 | 0.03 | |
| | | | | TH(+) | TH(-) | TH(+) | TH(-) | TH(+) | TH(-) | TH(+) | TH(-) | |
| | | | | Chrna6(+) | Chrna6(+) | Chrna6(-) | Chrna6(-) | Chrna6(+) | Chrna6(+) | Chrna6(-) | Chrna6(-) | |
| # cells-> | 524 | 305/524 | 219/524 | 188/305 | 50/305 | 17/305 | 50/305 | 150/219 | 21/219 | 34/219 | 14/219 | |
| fraction-> | | 0.58 | 0.42 | 0.62 | 0.16 | 0.06 | 0.16 | 0.68 | 0.10 | 0.16 | 0.06 | |
| | | | | TH(+) | TH(-) | TH(+) | TH(-) | TH(+) | TH(-) | TH(+) | TH(-) | |
| | | | | Chrb2(+) | Chrb2(+) | Chrb2(-) | Chrb2(-) | Chrb2(+) | Chrb2(+) | Chrb2(-) | Chrb2(-) | |
| # cells-> | 510 | 372/510 | 138/510 | 181/372 | 109/372 | 33/372 | 49/372 | 71/138 | 27/138 | 27/138 | 13/138 | |
| fraction-> | | 0.73 | 0.27 | 0.49 | 0.29 | 0.09 | 0.13 | 0.51 | 0.20 | 0.20 | 0.09 | |
| Lateral VTA | | | | | | | | | | | | |
| | Total | Slc17a6(+) | Slc17a6(-) | Slc17a6(+) | | | | Slc17a6(-) | | | | |
| | | | | TH(+) | TH(-) | TH(+) | TH(-) | TH(+) | TH(-) | TH(+) | TH(-) | |
| | | | | Chrna4(+) | Chrna4(+) | Chrna4(-) | Chrna4(-) | Chrna4(+) | Chrna4(+) | Chrna4(-) | Chrna4(-) | |
| # cells-> | 596 | 191/596 | 405/596 | 99/191 | 32/191 | 5/191 | 55/191 | 353/405 | 35/405 | 8/405 | 9/405 | |
| fraction-> | | 0.32 | 0.68 | 0.52 | 0.17 | 0.03 | 0.29 | 0.87 | 0.09 | 0.02 | 0.02 | |
| | | | | TH(+) | TH(-) | TH(+) | TH(-) | TH(+) | TH(-) | TH(+) | TH(-) | |
| | | | | Chrna6(+) | Chrna6(+) | Chrna6(-) | Chrna6(-) | Chrna6(+) | Chrna6(+) | Chrna6(-) | Chrna6(-) | |
| # cells-> | 534 | 177/534 | 357/534 | 50/177 | 50/177 | 3/177 | 74/177 | 256/357 | 65/357 | 19/357 | 17/357 | |
| fraction-> | | 0.33 | 0.67 | 0.28 | 0.28 | 0.02 | 0.42 | 0.72 | 0.18 | 0.05 | 0.05 | |
| | | | | TH(+) | TH(-) | TH(+) | TH(-) | TH(+) | TH(-) | TH(+) | TH(-) | |
| | | | | Chrb2(+) | Chrb2(+) | Chrb2(-) | Chrb2(-) | Chrb2(+) | Chrb2(+) | Chrb2(-) | Chrb2(-) | |
| # cells-> | 539 | 200/539 | 339/539 | 50/200 | 100/200 | 13/200 | 37/200 | 177/339 | 73/339 | 78/339 | 11/339 | |
| fraction-> | | 0.37 | 0.63 | 0.25 | 0.50 | 0.07 | 0.19 | 0.52 | 0.22 | 0.23 | 0.03 | |

Table S2. Related to Figure 2 – Expression of *Chrna4*, *Chrna6*, and *Chrb2* in VTA GABA neurons. Full quantification of triple channel mRNA FISH experiments is shown for medial (top section) and lateral VTA (bottom section). All sections were probed for *Gad2* and *Th*, while either *Chrna4*, *Chrna6* or *Chrb2* was probed in the 3rd channel.

| Medial VTA | | | | | | | | | | | | |
|-------------|-------|---------|---------|-----------|-----------|-----------|-----------|-----------|-----------|-----------|-----------|--|
| | Total | Gad2(+) | Gad2(-) | Gad2(+) | | | | Gad2(-) | | | | |
| | | | | TH(+) | TH(-) | TH(+) | TH(-) | TH(+) | TH(-) | TH(+) | TH(-) | |
| | | | | Chrna4(+) | Chrna4(+) | Chrna4(-) | Chrna4(-) | Chrna4(+) | Chrna4(+) | Chrna4(-) | Chrna4(-) | |
| # cells-> | 587 | 237/587 | 350/587 | 71/237 | 77/237 | 15/237 | 74/237 | 253/350 | 21/350 | 71/350 | 5/350 | |
| fraction-> | | 0.40 | 0.60 | 0.30 | 0.32 | 0.06 | 0.31 | 0.72 | 0.06 | 0.20 | 0.01 | |
| | | | | TH(+) | TH(-) | TH(+) | TH(-) | TH(+) | TH(-) | TH(+) | TH(-) | |
| | | | | Chrna6(+) | Chrna6(+) | Chrna6(-) | Chrna6(-) | Chrna6(+) | Chrna6(+) | Chrna6(-) | Chrna6(-) | |
| # cells-> | 620 | 252/620 | 368/620 | 57/252 | 120/252 | 6/252 | 69/252 | 298/368 | 51/368 | 14/368 | 5/368 | |
| fraction-> | | 0.41 | 0.59 | 0.23 | 0.48 | 0.02 | 0.27 | 0.81 | 0.14 | 0.04 | 0.01 | |
| | | | | TH(+) | TH(-) | TH(+) | TH(-) | TH(+) | TH(-) | TH(+) | TH(-) | |
| | | | | Chrb2(+) | Chrb2(+) | Chrb2(-) | Chrb2(-) | Chrb2(+) | Chrb2(+) | Chrb2(-) | Chrb2(-) | |
| # cells-> | 546 | 216/546 | 330/546 | 93/216 | 86/216 | 6/216 | 31/216 | 272/330 | 39/330 | 18/330 | 1/330 | |
| fraction-> | | 0.40 | 0.60 | 0.43 | 0.40 | 0.03 | 0.14 | 0.82 | 0.12 | 0.05 | 0.00 | |
| Lateral VTA | | | | | | | | | | | | |
| | Total | Gad2(+) | Gad2(-) | Gad2(+) | | | | Gad2(-) | | | | |
| | | | | TH(+) | TH(-) | TH(+) | TH(-) | TH(+) | TH(-) | TH(+) | TH(-) | |
| | | | | Chrna4(+) | Chrna4(+) | Chrna4(-) | Chrna4(-) | Chrna4(+) | Chrna4(+) | Chrna4(-) | Chrna4(-) | |
| # cells-> | 518 | 196/518 | 322/518 | 30/196 | 52/196 | 9/196 | 105/196 | 276/322 | 9/322 | 34/322 | 3/322 | |
| fraction-> | | 0.38 | 0.62 | 0.15 | 0.27 | 0.05 | 0.54 | 0.86 | 0.03 | 0.11 | 0.01 | |
| | | | | TH(+) | TH(-) | TH(+) | TH(-) | TH(+) | TH(-) | TH(+) | TH(-) | |
| | | | | Chrna6(+) | Chrna6(+) | Chrna6(-) | Chrna6(-) | Chrna6(+) | Chrna6(+) | Chrna6(-) | Chrna6(-) | |
| # cells-> | 467 | 174/467 | 293/467 | 33/174 | 79/174 | 6/174 | 56/174 | 254/293 | 22/293 | 15/293 | 2/293 | |
| fraction-> | | 0.37 | 0.63 | 0.19 | 0.45 | 0.03 | 0.32 | 0.87 | 0.08 | 0.05 | 0.01 | |
| | | | | TH(+) | TH(-) | TH(+) | TH(-) | TH(+) | TH(-) | TH(+) | TH(-) | |
| | | | | Chrb2(+) | Chrb2(+) | Chrb2(-) | Chrb2(-) | Chrb2(+) | Chrb2(+) | Chrb2(-) | Chrb2(-) | |
| # cells-> | 549 | 233/549 | 316/549 | 51/233 | 131/233 | 2/233 | 49/233 | 256/316 | 35/316 | 23/316 | 2/316 | |
| fraction-> | | 0.42 | 0.58 | 0.22 | 0.56 | 0.01 | 0.21 | 0.81 | 0.11 | 0.07 | 0.01 | |

Supplemental Experimental Procedures

Materials and Viral Vectors - AAV9.EF1a.ChR2-EYFP.WPRE.hGH, AAV9.EF1a.DIO.hChR2(H134R)-eYFP.WPRE.hGH and AAV9.EF1a.DIO.hChR2(H134R)-mCherry.WPRE.hGH were obtained from Penn Vector Core. AAV5.hSyn.DIO.hM4D(Gi)-mCherry.WPRE.hGH was from Addgene. AAV5/2.U6-control-sgRNA.hSyn.mCherry.WPRE.SV40pA (sgRNA target sequence: 5'-GCGAGGTATTCGGCTCCGCG-3') and AAV5/2.U6-Chrb2-sgRNA.hSyn.mCherry.WPRE.SV40pA (sgRNA target sequence: 5'-ATCAGCTTGTTATAGCGGGA-3') custom viruses were produced by Virovek, Inc. α -conotoxins were synthesized as previously described (Azam et al., 2010). Dihydro- β -erythroidine hydrobromide (DH β E), methyllycaconitine (MLA), picrotoxin, and atropine sulfate (atropine) were obtained from Sigma. 6-Cyano-7-nitroquinoxaline-2,3-dione (CNQX), 2,3-Dioxo-6-nitro-1,2,3,4-tetrahydrobenzo[*f*]quinoxaline-7-sulfonamide (NBQX), D-(-)-2-Amino-5-phosphonopentanoic acid (D-AP5), Octahydro-12-(hydroxymethyl)-2-imino-5,9,7,10a-dimethano-10aH-[1,3]dioxocino[6,5-d]pyrimidine-4,7,10,11,12-pentol (TTX), QX314 chloride (QX314), and galantamine hydrobromide (galantamine) were obtained from Tocris. Alexafluor (Alexa) 488 was obtained from Life Technologies. Green retrobeads IX were obtained from Lumafluor, Inc. PA-Nic was synthesized as previously described (Banala et al., 2018).

Stereotaxic Surgery - Male and female mice were used for surgery starting at 8 weeks of age. Mice were initially anesthetized with an intraperitoneal (i.p.) injection of a ketamine/xylazine mixture (120 mg/kg ketamine, 16 mg/kg xylazine). Mice were given additional "boost" injections of ketamine (100 mg/kg, i.p.) as needed. Alternatively, some mice were anesthetized with isoflurane: 3% (flow rate 500 mL/min) for induction and 1.5% (28 mL/min) for maintenance. Mice were secured into a stereotaxic frame and a small incision at the top of the head was made to expose the skull. Coordinates (unilateral) used for mVTA injections were (relative to bregma, in mm): M/L: +0.01 (or -0.01), A/P: -3.2, D/V: -4.55. Coordinates (bilateral) used for lateral VTA injections were (relative to bregma, in mm): M/L: \pm 0.5, A/P: -3.2, D/V: -4.75. Coordinates (bilateral) used for PPTg were (relative to bregma, in mm): M/L: \pm 1.20, A/P: -4.45, D/V: -4.05. Coordinates (unilateral) used for nucleus accumbens medial shell were (relative to bregma, in mm): M/L: \pm 0.5, A/P: +1.3, D/V: -4.75. Exact coordinates were adjusted to account for slight differences in the head size of individual mice: the bregma/lambda distance measured for each mouse was divided by the reported bregma/lambda distance for C57 mice (4.21), then multiplied by the A/P coordinate. The injection needle was slowly lowered through the drilled hole to the D/V coordinate. For AAV viruses, 500 nL of virus was infused at a rate of 50 nL/min. For bilateral retrobead infusions, 500 nL/hemisphere was infused at a rate of 50 nL/min. For all stereotaxic injections, the injection needle was left in place for 10 min after the infusion ended before slowly retracting the needle. Sutures were used to close the incision. At the conclusion of the surgery, mice were given ketoprofen (5 mg/kg, s.c.) and placed in a recovery cage, kept warm, and observed until they were ambulatory. Mice were single-housed following virus injection surgery and were given at least 14 days to recover and for the virus to express before beginning experimental procedures. For electrophysiology experiments, accurate targeting of VTA was determined via direct visualization of fluorescent neurons in brain slices during recordings.

Immunohistochemistry and Confocal Microscopy - Anti-GFP immunostaining and visualization with 3,3'-diaminobenzidine (DAB) of nAChR-GFP knockin/transgenic mouse brains (**Fig. S1a**) was performed as part of the same tissue analysis as we previously described (Shih et al., 2014). All other immunohistochemistry in the paper was performed as follows. Mice were anesthetized with sodium pentobarbital (200 mg/kg, i.p.) and transcardially perfused with 10 mL of heparin-containing phosphate buffered saline (PBS) followed by 30 mL of 4% paraformaldehyde. Brains were dissected and postfixed in 4% paraformaldehyde overnight at 4°C. Coronal brain slices (50 μ m) were cut on a freezing sliding microtome (SM2010R; Leica). VTA-containing slices were stained using the following procedure. Slices were first permeabilized for 2 min via incubation in PBST (0.3% Triton X-100 in PBS), followed by a 60 min incubation in blocking solution (0.1% Triton X-100, 5% horse serum in Tris-buffered saline (TBS)). Primary antibodies used in this study were as follows: sheep anti-TH (Millipore AB1542), rabbit anti-GFP (Invitrogen A11122), rabbit anti-DsRed (Clontech 632496), goat anti-ChAT (Millipore AB144P). Primary antibodies were diluted in blocking solution (anti-TH at 1:800, anti-GFP at 1:500, anti-DsRed at 1:500, anti-ChAT at 1:100). Slices were incubated in primary antibodies overnight at 4°C. Three 5 min washes in TBST (0.1% Triton X-100 in TBS) were done before transferring slices to secondary antibodies for a 60 min incubation at room temperature (anti-sheep or anti-rabbit Alexa 555, anti-rabbit Alexa 488, diluted to 1:500 in blocking solution). Slices were washed as before, mounted on slides, and coverslipped with Vectashield. Staining in the VTA was imaged as previously described (Mackey et al., 2012) with a Nikon A1 laser-scanning confocal microscope.

mRNA fluorescence in situ hybridization and image analysis - Mice were deeply anesthetized with sodium pentobarbital (200 mg/kg, i.p.) and decapitated. Brains were quickly removed on ice, snap frozen, and embedded in cryo-embedding medium (OCT). Brains were sectioned on a cryostat (CM3050; Leica) into 20 μm sections, sections were adhered to Superfrost[®] Plus slides, and kept at -20°C to dry for 60 min and stored at -80°C until use. Sections were fixed with 4% paraformaldehyde and processed for RNAscope (Advanced Cell Diagnostics) multichannel fluorescent *in situ* hybridization (FISH) according to the manufacturer manual for Multiplex assays. Sections were counterstained with DAPI for 30 s at room temperature. Probes for detection of specific targets (*Chrna4*, *Chrna6*, *Chrn2*, *Th*, *Slc17a6*, *Gad2*) were purchased from Advanced Cell Diagnostics (ACD; <http://acdbio.com/>). Probes for *Slc17a6*, *Gad2*, and *Th* were previously reported (Wallace et al., 2017; Xiao et al., 2017). Probes for *Chrna4*, *Chrna6*, and *Chrn2* were validated by comparing co-expression of TH/nAChR subunit mRNA with previously reported analyses using labeled riboprobes (Azam et al., 2002). This prior study indicated that 80-90% of *Th*(+) neurons also expressed *Chrna4*, *Chrna6*, and *Chrn2*. Consistent with this, we found that 97%, 88%, and 88% of *Th*(+) neurons in lateral VTA were also positive for *Chrna4*, *Chrna6*, and *Chrn2*, respectively (Fig. S2).

Sections were imaged on a Nikon A1 confocal microscope according to the following parameters: 1024 x 1024 pixels, ~ 200 nm/pixel, 20x 0.75 NA objective. Nikon system images containing 3 or 4 channels were processed with custom scripts in ImageJ (NIH). All images to be used for FISH quantification were acquired and processed in the same manner. FISH quantification employed the “fluorescence coverage (%)” method (Wallace et al., 2017), which reports the fraction of fluorescent pixels to total pixels in a cellular region of interest (ROI). Multichannel images were opened and all channels (including Dapi staining to identify cellular locations) were overlaid. Background subtraction was performed on each channel separately, as follows. Each channel in multichannel images were opened and background was measured in ImageJ in an area of the image devoid of cells as indicated by Dapi staining. Background values for each channel were subtracted to form a new background-subtracted channel image. Using the background-subtracted image, ROIs were drawn manually around cells containing at least one fluorescent signal, and Dapi staining assisted in distinguishing individual cells from cell clusters. A binary image was then produced for each channel for quantitative analysis using the default algorithm in ImageJ (version 1.51n). The percentage of fluorescent pixels to total pixels within each ROI was determined. These data were used to create x vs. y plots of percent coverage for each probe/channel and each cell. To assign a cell as either positive or negative for expression of each probe, a percent coverage “cutoff” was used such that the percent coverage in a ROI had to meet or exceed the cutoff to be counted as positive for the probe. Cutoffs were determined *de novo* for each assay and imaging session to account for any differences in probe performance or tissue autofluorescence over time or across days. A minimum of 3 mice were sampled for each condition, and 3-6 images were analyzed per mouse and per VTA sub-region (medial vs. lateral VTA).

Brain Slice Preparation and Recording Solutions - Brain slices were prepared as previously described (Engle et al., 2012). Mice were anesthetized with Euthasol (sodium pentobarbital, 100 mg/kg; sodium phenytoin, 12.82 mg/kg) before trans-cardiac perfusion with oxygenated (95% O_2 /5% CO_2), 4°C N-methyl-D-glucamine (NMDG)-based recovery solution that contains (in mM): 93 NMDG, 2.5 KCl, 1.2 NaH_2PO_4 , 30 NaHCO_3 , 20 HEPES, 25 glucose, 5 sodium ascorbate, 2 thiourea, 3 sodium pyruvate, 10 $\text{MgSO}_4 \cdot 7\text{H}_2\text{O}$, and 0.5 $\text{CaCl}_2 \cdot 2\text{H}_2\text{O}$; 300-310 mOsm; pH 7.3-7.4). Brains were immediately dissected after the perfusion and held in oxygenated, 4°C recovery solution for one minute before cutting a brain block containing the VTA and sectioning the brain with a vibratome (VT1200S; Leica). Coronal slices (200-250 μm) were sectioned through the VTA and transferred to oxygenated, 33°C recovery solution for 12 min. Slices were then kept in holding solution (containing in mM): 92 NaCl, 2.5 KCl, 1.2 NaH_2PO_4 , 30 NaHCO_3 , 20 HEPES, 25 glucose, 5 sodium ascorbate, 2 thiourea, 3 sodium pyruvate, 2 $\text{MgSO}_4 \cdot 7\text{H}_2\text{O}$, and 2 $\text{CaCl}_2 \cdot 2\text{H}_2\text{O}$; 300-310 mOsm; pH 7.3-7.4) for 60 min or more before recordings.

Brain slices were transferred to a recording chamber being continuously superfused at a rate of 1.5-2.0 mL/min with oxygenated 32°C recording solution. The recording solution contained (in mM): 124 NaCl, 2.5 KCl, 1.2 NaH_2PO_4 , 24 NaHCO_3 , 12.5 glucose, 2 $\text{MgSO}_4 \cdot 7\text{H}_2\text{O}$, and 2 $\text{CaCl}_2 \cdot 2\text{H}_2\text{O}$; 300-310 mOsm; pH 7.3-7.4). For all recordings, the recording solution was supplemented with 1 μM atropine to eliminate contributions from muscarinic ACh receptors. Patch pipettes were pulled from borosilicate glass capillary tubes (IB150F-4; World Precision Instruments) using a programmable microelectrode puller (P-97; Sutter Instrument). Tip resistance ranged from 5.0 to 10.0 $\text{M}\Omega$ when filled with internal solution. The following internal solution was used (in mM): 135 potassium gluconate, 5 EGTA, 0.5 CaCl_2 , 2 MgCl_2 , 10 HEPES, 2 MgATP , and 0.1 GTP; pH adjusted to 7.25 with Tris base; osmolality adjusted to 290 mOsm with sucrose. For uncaging, this internal solution also contained QX-314 (2 mM) for improved voltage control.

Standard Patch Clamp Electrophysiology - Neurons within brain slices were first visualized with infrared or visible differential interference contrast (DIC), followed in some cases by fluorescence microscopy to identify neurons expressing fluorescent proteins or within range of fluorescent axons. Electrophysiology experiments were conducted using a Nikon Eclipse FN-1 or Scientifica SliceScope. A computer running pCLAMP 10 software was used to acquire whole-cell recordings along with a Multiclamp 700B or Axopatch 200B amplifier and an A/D converter (Digidata 1440A or Digidata 1550A). pClamp software, Multiclamp/Axopatch amplifiers, and Digidata A/D converters were from Molecular Devices. Data were sampled at 10 kHz and low-pass filtered at 1 kHz. Immediately prior to gigaseal formation, the junction potential between the patch pipette and the superfusion medium was nulled. Series resistance was uncompensated. A light emitting diode (LED) light source (XCite 110LED; Excelitas) coupled to excitation filters (400/40 nm, 470/40 nm, and 560/40 nm bandpass) was used to search for fluorescent neurons and, for optogenetic experiments involving ChR2, to stimulate the preparation with light flashes. Light flashes were triggered by pCLAMP via TTL pulses. Flash energy output from the LED was determined by calibration using a photodiode power sensor (Model S120C; Thor Labs). Optical pulse duration (0.5-5 ms) and flash strength (<0.01 mW/mm²) were empirically chosen for each cell such that baseline responses were initially ~50-150 pA. Optical pulse duration and flash strength were longer/stronger (20 s, 0.12 mW/mm², respectively) for evoking ACh release from PPTg axons.

To record physiological events following local application of drugs, a drug-filled pipette was moved to within 20-40 μ m of the recorded neuron using a second micromanipulator. A Picospritzer (General Valve) dispensed drug (dissolved in recording solution) onto the recorded neuron via a pressure ejection. Ejection volume, duration, and ejection pressure varied depending on the goal of the experiment. Approximate ejection pressures (in p.s.i.) for dispensing saturating ACh concentrations, ACh concentrations for testing galantamine potentiation, and PA-Nic application were 12, 2, and 2, respectively.

2-Photon Laser Scanning Microscopy, Electrophysiology, and Nicotine Uncaging - PA-Nic photolysis was performed as previously described (Banala et al., 2018). An Olympus BX51 upright microscope and a 60x (1.0 NA) objective was used to visualize cells. Prairie View 5.4 (Bruker Nano) software was used for image acquisition, photostimulation, and electrophysiology acquisition via a Multiclamp 700B patch clamp amplifier. Analog signals were sampled at 5 kHz and low-pass filtered at 1 kHz, and an A/D converter (PCI-NI6052e; National Instruments) was used for digitization. Patch clamp recordings were carried out using the internal solution mentioned above, except that Alexa 488 or 568 (100 μ M) was also included in the recording pipette to visualize cells using 2-photon laser scanning microscopy. After break-in, the internal solution with the Alexa dye was allowed to equilibrate for 15-20 min before imaging was initiated. A Mai Tai HP1040 (Spectra Physics) was used to excite Alexa 488 or 568. Images in **Fig. 1b-d** were acquired by sequentially tuning and imaging, first at 920 nm to image Alexa 488 followed by 1040 nm to image tdT. Alexa 568 was used for cell imaging at 790 nm during uncaging experiments. The laser was pulsed at 90 MHz (~250 fs pulse duration), and a M350-80-02-BK Pockels cell (ConOptics) was used for power attenuation. The dual-channel, 2-photon fluorescence was detected by two non-de-scanned detectors; green and red channels (dual emission filters: 525/70 nm and 595/50 nm) were detected by the following Hamamatsu photomultiplier tubes (PMTs), respectively: end-on GaAsP (7422PA-40) and side-on multi-alkali (R3896). A 405 nm continuous wave laser (100 mW OBIS FP LX; Coherent) was used for photostimulation/uncaging via a second set of x-y galvanometers incorporated into the scanhead (Cambridge Technologies). 405 nm laser power was measured below the sample but above the condenser using a Field Master GS (LM10 HTD sensor head). PA-Nic (2 mM) was applied locally to the recorded cell via a large-bore (30-40 μ m diameter) pressure ejection pipette at low pressure. The Markpoints module of Prairie View 5.4 software was used to select spots in the field of view (~1 μ m diameter) for focal uncaging of nicotine via 405 nm laser light flashes (50 ms, 1-2 mW).

Supplemental References

Azam, L., Maskos, U., Changeux, J.P., Dowell, C.D., Christensen, S., De Biasi, M., and McIntosh, J.M. (2010). α -Conotoxin BuIA[T5A;P6O]: a novel ligand that discriminates between $\alpha 6\beta 4$ and $\alpha 6\beta 2$ nicotinic acetylcholine receptors and blocks nicotine-stimulated norepinephrine release. *FASEB J* 24, 5113-5123.

Azam, L., Winzer-Serhan, U.H., Chen, Y., and Leslie, F.M. (2002). Expression of neuronal nicotinic acetylcholine receptor subunit mRNAs within midbrain dopamine neurons. *J Comp Neurol* 444, 260-274.

Banala, S., Arvin, M.C., Bannon, N.M., Jin, X.T., Macklin, J.J., Wang, Y., Peng, C., Zhao, G., Marshall, J.J., Gee, K.R., *et al.* (2018). Photoactivatable drugs for nicotinic optopharmacology. *Nat Methods* 15, 347-350

Engle, S.E., Broderick, H.J., and Drenan, R.M. (2012). Local application of drugs to study nicotinic acetylcholine receptor function in mouse brain slices. *J Vis Exp*, e50034.

Mackey, E.D., Engle, S.E., Kim, M.R., O'Neill, H.C., Wageman, C.R., Patzlaff, N.E., Wang, Y., Grady, S.R., McIntosh, J.M., Marks, M.J., *et al.* (2012). $\alpha 6^*$ Nicotinic Acetylcholine Receptor Expression and Function in a Visual Salience Circuit. *J Neurosci* 32, 10226-10237.

Shih, P.Y., Engle, S.E., Oh, G., Deshpande, P., Puskar, N.L., Lester, H.A., and Drenan, R.M. (2014). Differential expression and function of nicotinic acetylcholine receptors in subdivisions of medial habenula. *J Neurosci* 34, 9789-9802.

Wallace, M.L., Saunders, A., Huang, K.W., Philson, A.C., Goldman, M., Macosko, E.Z., McCarroll, S.A., and Sabatini, B.L. (2017). Genetically Distinct Parallel Pathways in the Entopeduncular Nucleus for Limbic and Sensorimotor Output of the Basal Ganglia. *Neuron* 94, 138-152.

Xiao, L., Priest, M.F., Nasenbeny, J., Lu, T., and Kozorovitskiy, Y. (2017). Biased Oxytocinergic Modulation of Midbrain Dopamine Systems. *Neuron* 95, 368-384.